NOVA SCHOOL OF SCIENCE & TECHNOLOGY

DEPARTAMENT OF MATERIAL SCIENCES

Jaime Silveira Viegas

BSc in Micro and Nanotechnology Engineering

Solution-processed oxide thin films for electrochromic devices application

MASTER IN Micro and Nanotechnology Engineering

NOVA University Lisbon

September, 2024

DEPARTAMENT OF
MATERIAL SCIENCES

Solution-processed oxide thin films for electrochromic devices application

Jaime Silveira Viegas

BSc in Micro and Nanotechnologies Engineering

Adviser: Dr. Rita Branquinho
Assistant Professor, NOVA School of Science and Technology

Co-advisers: Dr. Emanuel Carlos
Assistant Researcher, NOVA School of Science and Technology

Examination Committee:

Chair: Dr. Hugo Águas,
Associate Professor, NOVA School of Science and Technology

Rapporteurs: Dr. Joana Vaz Pinto
Assistant Professor, NOVA School of Science and Technology

Adviser: Dr. Rita Branquinho,
Assistant Professor, NOVA School of Science and Technology

MASTER IN MICRO AND NANOTECHNOLOGY ENGINEERING

NOVA University Lisbon
September, 2024

Solution-processed oxide thin films for electrochromic devices application

ACKNOWLEDGMENTS

Firstly, i express my gratefulness to the institution that embraced me for the last five years, NOVA School of Science and Technology, especially to the Department of Material Sciences.
Secondly, a special thank you to my supervisors Dr. Rita Branquinho and Dr. Emanuel Carlos, for their incredible patience to guide me. Their knowledge and guidance were essential to complete this challenging work.
To the people of CENIMAT and CEMOP, who provided me with the formations to use the equipment and helped me every time i asked.
I cannot put into words how thankful i am to all the teachers that were part of my life, from the first cycle to the university, from the ones who taught me how to read to the ones who introduced me to nanotechnologies, learning was always a big pleasure of mine and i look forward continuing to do it. A particular thank you to Mrs. Mirna, who taught me everything i know about the English language, i could not have written this document without those years of intensive learning.
Another big thank you to my friends, they were always there ready to share a laugh and have always helped me to relax during stressful moments.
Finaly, a warm thank you to my family, they have always provided me everything i needed to finish my studies. A special thank you to my grandfather, whose company and great abilities to grill fish were essential to give me the final confidence and energy to finish this work.
This work was financed by national funds from FCT - Fundação para a Ciência e a Tecnologia, I.P., in the scope of the projects LA/P/0037/2020, UIDP/50025/2020 and UIDB/50025/2020 of the Associate Laboratory Institute of Nanostructures, Nanomodelling and Nanofabrication – i3N).

" So, to work now! Lift up your hammers!”
Guiseppe Verdi, in “Il Trovatore”

ABSTRACT

Electrochromic (EC) devices allow to reversibly change their colour when a small voltage is applied and can be used in buildings, satellites or airplanes. NiO and WO_3 are two promising electrochromic materials with great electrochromic properties. Once NiO is a cathodic and WO_3 is an anodic EC material, it is beneficial to combine them in a complementary effect electrochromic window. The production techniques of both NiO and WO_3 devices have been evolving but are still expensive due to typical vacuum-based and high pressure production processes. Therefore, it is highly important to find new low-cost methods that can allow to produce EC films with good electrochromic properties. Solution combustion synthesis (SCS) is a simple low-cost method and a possible alternative. In this work, NiO and WO_3 films were produced through SCS and deposited by spin coating. Once the film production was optimized, they were structurally, optically and electrochemically characterized. NiO and WO_3 films presented a thickness of (195±6) nm and of (53±3) nm, respectively. Both films did not present long range order and only NiO films presented a porous structure. WO_3 and NiO films presented an identical optical modulation of 20%. Cyclic voltammetry measures revealed two oxidation and two reduction peaks for NiO films and only one reduction peak for WO_3. Finally, NiO and WO_3 films presented low operating voltages and coloration/bleaching times of (21±1)/(8±1) s and (45±7)/ (46±4) s, respectively. The films exhibited a promising reversible electrochromic behaviour which can be employed in complementary effect electrochromic windows after process optimization.

Keywords: Electrochromic, Nickel Oxide, Tungsten Oxide, Spin Coating, Solution Combustion Synthesis.

RESUMO

Os dispositivos electrocrómicos mudam reversivelmente de cor quando uma pequena tensão é aplicada nos seus terminais, podendo ser usados em edifícios, satélites ou aviões. NiO e WO_3 são dois materiais electrocrómicos promissores que sendo, respetivamente, catódico e anódico, podem ser combinados numa janela electrocrómica de efeito complementar. Os métodos de fabrico de dispositivos à base destes materiais têm vindo a evoluir, mas como ainda assentam em processos de vácuo e altas pressões, permanecem os altos custos de produção. Assim, torna-se importante encontrar métodos *low-cost* que permitam produzir dispositivos com boas propriedades electrocrómicas. A síntese por combustão (SCS) apresenta-se como um método simples e de baixo custo. Neste trabalho filmes de NiO e WO_3 foram produzidos por SCS e depositados por spin coating. Após otimização do processo de fabrico, os filmes foram estruturalmente, opticamente e electroquimicamente caracterizados. Os filmes de NiO apresentaram uma espessura de (195±6) nm e os de WO_3 de (53±3) nm. Os filmes não apresentaram ordem a longas distâncias e apenas os filmes de NiO apresentaram uma estrutura porosa. Os filmes de WO_3 e de NiO apresentaram uma modulação ótica semelhante, de cerca de 20%. As medidas de volumetria cíclica revelaram a presença de dois picos de redução e dois picos de oxidação para os filmes de NiO, mas apenas um pico de redução foi registado para o filme de WO_3.. Por fim, os filmes de NiO apresentaram tempos de coloração/ descoloração de (21±1)/(8±1) s e os de WO_3 (45±7)/ (46±4) s. Desta forma tanto os filmes de NiO como os de WO_3 exibiram um comportamento electrocrómico reversível, podendo ser usados em janelas electrocrómicas após otimização do processo de fabrico.

Palavras chave: eletrocromismo, Óxido de Níquel, Óxido de Tungsténio, Spin Coating, Síntese por Combustão

CONTENTS

LIST OF FIGURES

List of Tables

GLOSSARY

Electrochromism	A phenomenon in which a material displays changes in colour or transparency
Transmittance	Ratio of the light energy falling on a body to that transmitted through it
Optical Modulation	Difference of transmittance between coloured and bleaching states

.

ACRONYMS

EC	Electrochromic device
ISL	Ion Storage Layer
ECL	Electrochromic Layer
TMOs	Transition Metal Oxides
SCS	Solution combustion Synthesis
ITO	Indium thin oxide
FTO	Fluorine doped thin oxide
CE	Coloration efficiency
FTIR-ATR	Fourier Transform Infrared Total Reflectance-Attenuated Total Reflectance
SEM	Scanning Electron Microscopy
XRD	X Ray Diffraction
IPCC	International Panel on Climate Change
OV	Oxidising Valence
RV	Reducing Valence

SYMBOLS

ϕ	Reducer/oxidizer ratio
$t_{c\ 90\%}$	Coloration time
$t_{b\ 90\%}$	Bleaching time
ΔT	Optical modulation

MOTIVATION

One of the biggest challenges of the 21st century is the threat of climate change. According to the Intergovernmental Panel on Climate Change (IPCC), global warming may lead to an increase of earth's average temperature 1.5 ºC above pre-industrial levels [1]. One of the challenges science must address is the thermal isolation of buildings, since they consume a large portion of the total energy that is produced. Around 30% of a building's energy is lost by windows, therefore it is necessary to find new technologies that can help mitigate this energy loss [2]. Electrochromic devices are promising candidates, since they are designed to reversibly change their transmittance and colour when a small voltage is applied, they take less energy consumption. There are a wide variety of applications where they can be employed like information displays, thermal control of satellites and smart windows, leading to more energy efficient buildings, satellites or even airplanes. The main objective of this work is to produce NiO and WO_3 thin films by solution combustion synthesis and to study their electrochromic behaviour and application in electrochromic devices.

Figure i- Electrochromic Window produced by Wglass

1

INTRODUCTION

The first reports of electrochromism were published in 1953 at the Blazers AZ, where colour changes were observed when immersing WO_3 films in sulfuric acid [3]. In 1969 *Deb* created the first electrochromic (EC) device using WO_3, but during the second half of the 1970s, liquid crystals started to dominate the market [3]. Later, in 1980, the energy efficiency of EC devices highlighted their potential and new developments were made in the field, at the same time NiO EC films started to be developed [3]. The evolution continued and these devices are now widely present on the market and can be seen in diverse applications such as airplanes, buildings and satellites [4].

1.1 Structure and materials of EC devices

Figure 1.1 presents the basic configuration of an EC device: substrate/transparent conductor/ EC film/ electrolyte/ counter electrode. In order to achieve colouration, an electrical field is applied between the counter electrode and the transparent conductor, leading to the oxidation/reduction of the EC film trough the insertion/extraction of ions from the electrolyte, changing its optical bandgap and consequently its colour [5]. Cathodic EC materials achieve coloration trough ion insertion (electrochemical reduction), while anodic EC materials trough ion extraction (electrochemical oxidation)[6].

For real life applications, EC films are, often, incorporated in a 5 layer EC device where the counter electrode is an ion storage layer (ISL), also deposited over a transparent conductor and a substrate [5]. The ISL can also consist of an EC film, in this case the removal of electrons from the ISL layer will change its colour. Once both ISL and ECL will change their colour, there is colour overlay, this phenomenon is called complementary effect [4].

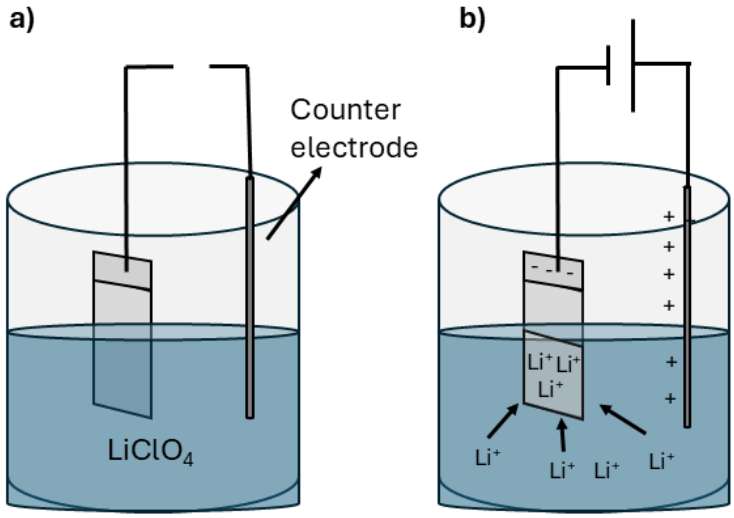

Figure 1.1- EC mechanism of a cathodic Electrochromic film with a) no voltage applied b) a voltage applied

Transparent conductors allow insertion/extraction of charges into the device and are usually tin doped indium oxide (ITO) or fluorine doped tin oxide (FTO) [4].

The performance on an EC film vastly depends on the electrolyte. Its main function is as source of ionic species and to allow ionic conductivity. Therefore, the performance will depend on the size, volume and diffusion kinetics of the electrolyte ions [7]. Li^+ based electrolytes are widely used due to their fast diffusion assured by the small ionic radius of Li ions, but still remain expensive, unsafe and rely on a critical raw material [7]. Non-metal H^+ have an even smaller ionic radius, with faster diffusion times, yet corrosion and hydrogen leakage have led to poor durability and unstable performance of the devices [7]. Electrolytes based on Na^+ and K^+ ions have emerged due to their safety and abundance, but their large ionic radius does not make them attractive for EC device fabrication [7]. Multi valent ion based electrolytes (like Zn^{2+}, Ca^{2+}, Al^{3+}, Mg^{2+}) are another alternative that takes advantage of the multiple ions that can be involved in the reaction, increasing the switching speed of a device, however strong electrostatic interactions between the inserted ions and the host materials lead to poor cyclic stability and low optical contrast, therefore it is not a popular alternative [7].

To evaluate the EC performance of a device it is important to consider several parameters, such as optical modulation, switching time and coloration efficiency[6]. Optical modulation refers to the difference of transmittance in coloured and bleached states [6]. Switching Time evaluates the time needed to switch from coloured to bleached state and from bleached to colour state, usually it is measured when there is an optical change of 90%[6]. Coloration efficiency (CE) helps understanding the efficiency of the colouring/bleaching process and is defined as the optical modulation per injected charge per unit area [6]. To assure fast switching times both

the electrolyte and the EC film should have high ionic conductivity [4]. The EC film must also present high electronic conductivity, large optical transmittance, high coloration efficiency and cyclic durability[4].

The performance of an EC device depends on several factors like the EC film surface area, crystallinity, electrical conductivity, porosity and roughness [2], [8]. One of the main parameters that has a great influence on the EC properties is the surface area. Higher surface areas increase the space available for ion-film reactions, decreasing the diffusion length of the electrolyte ions and, consequently decreasing coloration/bleaching times [6]. Crystallinity has a strong Influence on the surface area of the films. Amorphous films tend to have more surface area available than crystalline films due to the lack of long range order, improving ion insertion/extraction and increasing the switching speed [8]. On the other hand, crystalline films have better adhesion to the substrate and are more stable [8]. The porosity of the films and the existence of microstructures are other factors that can increase the surface area, enhancing the performance of the device[2], [8].

Several materials have been used to produce EC films, but transition metal oxides (TMOs) have become a popular choice due to their high chemical stability, high electrochemical activity and appropriate potential window [2].

NiO has been widely used as an anodic metal oxide due to its compatibility with EC windows, low-cost and ease of preparation, but their low conductivity, optical modulation and life cycle are still drawbacks that need to be addressed [2]. Among the several techniques (sputtering, sol gel, hydrothermal, solvothermal, spin coating) that have been reported ,(table 1.1), NiO films produced by hydrothermal synthesis have shown good results with high optical modulation, 70 % (600 nm), good cycling stability, and small coloration/bleaching times, 5/7s [9], [10], [11], [12], [13]. Although hydrothermal synthesis may allow to produce films with microstructures, its high pressure and high temperature requirements are not attractive for large scale production [2].

WO_3 has become a promising cathodic metal oxide due to its high optical modulation, high colouring efficiency, short switching times and low cost [8]. However, its cycling stability is still insufficient for some applications and expensive techniques like solvothermal and sputtering continue to dominate its fabrication method [8]. As shown in table 1.1, hydrothermal, self assembly, spray coating, vacuum evaporation and APCVD are among several techniques reported to produce WO_3 EC films, [14], [15], [16], [17], [18]. There are reports of sputtering made WO_3 films with controllable crystallinity, high optical modulations, 73 % (1000 nm), small coloured/bleaching times, 5/3 s, and high CE, 81 $Cm^2.C^{-1}$ [19]. *Y.Yao* reported WO_3 crystalline

quantum dots made by spray coating with high optical modulation, 98% (633 nm), fast coloration/bleaching times, 5/4 s, high CE of 77 $Cm^2.C^{-1}$ and excellent cycling stability (3000 cycles with 10% optical loss) [18]. The mass production of both NiO and WO_3 still rely on high-cost methods, therefore it is important to study a low-cost production technology that can allow to produce high efficiency NiO and WO_3 electrochromic films [2], [8]. Techniques like Inkjet printing and self assembly have produced WO_3 films with higher CE values but with lower optical modulations and higher colour/bleaching times [16], [17]. As shown in table 1.1, although good results have been obtained by solution techniques, the performance of WO_3 and NiO solution-based films is still lower than the obtained through vacuum based techniques. Therefore, it is highly important to improve the EC performance of solution based WO_3 and NiO films, helping lower the costs of mass production.

1.2 Solution Combustion Synthesis

Solution combustion synthesis (SCS) is a possible alternative method that can help lowering the production costs of NiO and WO_3 EC films [20], [21], [22]. This method is based on an exothermic redox reaction between a metal precursor and a fuel. The metal precursor will receive electrons from the fuel and the metal oxides will be produced [23]. To trigger the combustion, it is necessary to provide a certain temperature to the precursor solution, (ignition temperature), leading to a strong exothermic reaction. Being a low temperature process, it can be seen has a greener alternative to typical fabrication methods of EC films that evolve higher temperatures, high pressures (hydrothermal synthesis) or vacuum (sputtering) [23].
The final properties of the produced thin films will depend on the reaction parameters like the fuel (reducer), the metal source (oxidizer), the reducer to oxidizer ratio (ϕ), the initiation type, the ph of the precursor solution and the atmosphere environment [23].

$$\text{Metal precursor} + \text{Fuel} + \text{Solvent} \longrightarrow \text{Metal Oxide} + H_2O + CO_2 + N_2$$

There are some reports of NiO EC films made by SCS [20], [22]. A recent study reported NiO spin coated films made by SCS using nickel nitrate as metal source (oxidizer) and thiourea as fuel (reducer), with good optical modulation, 60% (550 nm), but with low colour efficiency, 26 $Cm^2.C^{-1}$, and high colouration time, 12s [22].
Similarly to NiO, WO_3 films have also been produced through SCS [21]. A recent work produced WO_3 spin coated films with different thicknesses using WCl_6 as metal source, acetic acid as fuel

and hydrogen peroxide as chelating agent. The best results had an optical modulation of 40% (633 nm), a coloration efficiency of 35 $cm^2.C^{-1}$ and coloration/bleaching times of 32/10 [21]. In this work SCS was used to produce both WO_3 and NiO thin films, their properties and application in EC devices were evaluated.

Table 1.1- State of the art of NiO and WO3 electrochromic devices.

	Method	Electrolyte	CE ($Cm^2.C^{-1}$)	ΔT (%)	Coloration/ Bleaching Times (s)	Ref
WO_3	Sol Gel	1M LiClO4-PC	56	56 (633 nm)	6/3	[24]
	Combustion	1 M LiI-PEG	35	40 (633 nm)	32/10	[21]
	Spray Coating	0.2 MLiClO4-PC	77	98 (633 nm)	5/4.0	[18]
	Inkjet Printing	61:17:7:15 ACN:PC:LiClO4:PMMA	132	75 (633 nm)	10/13	[17]
	Self assembly	0.1M LiClO4-PC	121	61 (1060 nm)	86/78	[16]
	Hydrothermal	1M LiClO4-PC	57	78 (630 nm)	5/6	[15]
	Solvothermal	1M H2SO4	75	75 (630 nm)	7/2	[14]
	Sputtering	1M LiClO4-PC	81	73 (1000 nm)	5/3	[19]
NiO	Sputtering	1 M PC-LiClO4	24	55 (-)	10/4	[13]
	Sol Gel	1 M KOH	71	51 (550 nm)	-	[12]
	Hydrothermal	1 M LiOH	57	70 (600 nm)	5/7	[10]
	Solvothermal	1 M KOH	31	64 (550nm)	12/10	[9]
	Spray Pyrolysis	0.5 M PC-LiClO4	31	39 (550 nm)	8/2	[11]
	Combustion	1 M NaOH	26	60 (550 nm)	12/4	[22]
		1 M $LiClO_4$	92	55 (550 nm)	17/2	[20]

2

MATERIALS AND METHODS

With the aim of understanding the EC performance of combustion based WO_3 and NiO thin films, precursor solutions of both materials were prepared by SCS and deposited by spin-coating. This process was optimized, and the thin films were properly characterized.

2.1 WO_3 and NiO precursor solutions preparation

To prepare the NiO precursor solution, 0.29 g of nickel (II) nitrate, $N_2NiO_6.6H_20$, (Sigma-Aldrich, CAS:13478-00-7) were dissolved in 10 ml of 2-methoxyethanol, $CH_3OCH_2CH_2OH$, (Sigma-Aldrich, CAS:109-86-4) in a concentration of 0.1 M. To complete the exothermic reaction, 0.1 g of urea, CH_4N_2O, (Fisher Chemical, CAS:57-13-6) was added and the mixture was left stirring. To prepare the WO_3 precursor solution, 1g of tungsten hexachloride, WCl_6, (Sigma-Aldrich, CAS:13283-01-7,>=99.9%) was dissolved in 10 ml ethanol absolute, C_2H_6O, (Merck, CAS:64-17-5), in a concentration of 0.18 M. Afterwards, 2 ml of acetic acid, CH_3CO_2H, (Merck, CAS:64-19-7, 99%) was added to the mixture and the solution was left stirring for 30 minutes. To finalize, 2 ml of hydrogen peroxide, H_2O_2, (Panreac AppliChem, CAS:7722-84-1, 30%) was added and the solution was left stirring at 40 ºC for 2 hours. The stoichiometric calculations for both reactions are presented in annex A1.

2.2 WO_3 and NiO thin films production and characterization

The NiO and WO3 precursor solutions were deposited by spin-coating on silicon, glass and ITO/glass substrates to produce the respective thin films. Prior to deposition, all silicon and glass substrates were cleaned in an ultrasonic bath, in acetone, in isopropanol and in water

during 15 minutes each stage, followed by exposure to UV/Ozone in a PSD-UV Novascan system, with a lamp distance of 3 cm.

Immediately after exposure, 8 layers of each film were deposited by spin coating (Laurell). Each deposition had a duration of 35 seconds at 3000 rpm and an acceleration of 2000 rpm, followed by immediate annealing in a hot plate at 300 ºC, for 5 minutes between layers and a final annealing step of 1 hour. To allow the necessary access to the conductive ITO contact two methods were used; i) a small region of the ITO/glass was covered with kapton tape prior to the deposition, ii) no tape was used prior to spin-coating and the oxide thin film was exposed after deposition, by chemical etching with HCl (Merck, CAS:7647-01-0, 37%) using kapton tape as a mask to protect the film.

To assist the chemical etching, a study of the annealing time influence in the ITO resistance was performed. For that purpose, one ITO/glass sample was submitted to the same annealing procedure used for the film production and a second sample without the final 1h annealing step. The resistance of the ITO contact was measured with a multimeter.

The film's thickness was measured with a profilometer Ambios XP-Plus 200 Sylus. X-ray measurements were made from 10º to 60º with a Malvern Panalytical Aeris to understand the crystallographic structure of the films, while SEM analysis was made with a SEM Hitachi Regulus SU8220 to understand their crystallographic structure.

FTIR-ATR analysis was made with the Si samples in order to understand if there was a complete conversion to metal oxide.

To study the transmittance of the films, spectrophotometer, (Perkin Elmer lambda 950 UV-VIS-NIR), measurements were made from 200 nm to 800 nm, in the original, coloured and bleaching states. The coloured and bleaching states were obtained by applying voltages with a potentiostat (Gamry Ref 600). The same system was used to obtain cyclic voltammetry curves, applying voltages between -1 V and 1.5 V for NiO films and -1.5V and 1 V for WO_3, with a scan rate of 50 $mV.s^{-1}$. Chronoamperometry measurements were also made, with the help of an Ocean Optics portable spectrophotometer, to extract the ON-OFF cycles, by applying voltages of -0.5V and 1 V during 90s each for NiO and of -0.5 and -0.25 for the same period for WO_3 films.

To perform the electrical measurements as well as to achieve the coloured and bleaching states, a $LiClO_4$ electrolyte, (C=0.1M), was in contact with a platinum counter electrode and a reference electrode (Ag/AgCl). To prepare the electrolyte, lithium perchlorate, $LiClO_4$, (Sigma Aldrich, CAS: 7791-03-9, >=98%), was added to Propylene Carbonate, $C_4H_6O_3$, (Acros Organics, CAS: 108-32-7, >95%) and left stirring until it was completely dissolved.

3

RESULTS AND DISCUSSION

The obtained results are presented in the following chapter. Firstly, it is presented the difference between the devices produced whit kapton tape during spin coating and the devices where the ITO contact was produced through chemical etching. Secondly, the characterization results of the optimized films are exposed and discussed.

3.1 NiO and WO_3 solution preparation and film deposition

A brief resume of the steps followed to produce the NiO and WO_3 precursor solutions and EC films is presented in figure 3.1.

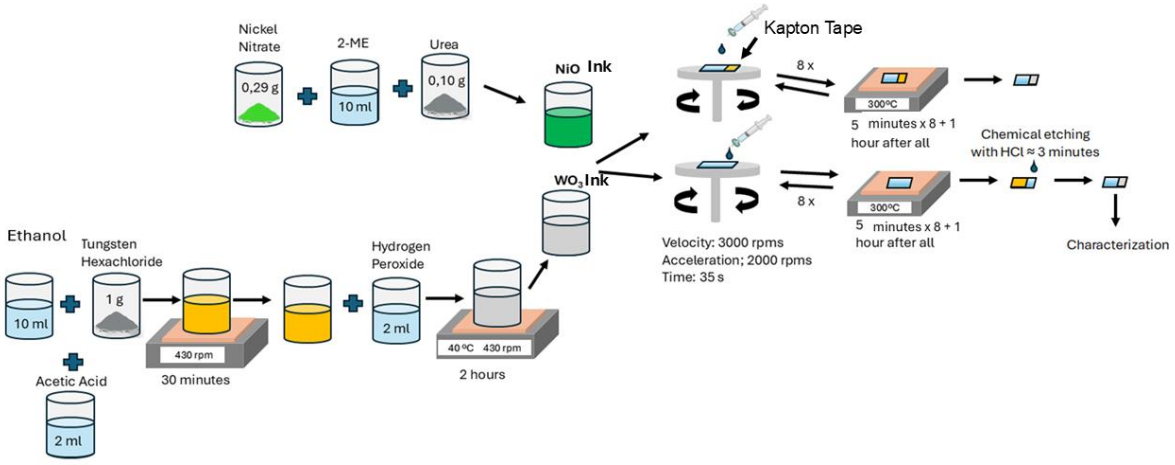

Figure 3.1- Schematic of the steps followed for NiO and WO_3 EC film production

In order to colour/bleach the device, it was essential to maintain an ITO contact that could allow the application of a voltage and lead to ion insertion/extraction. To preserve an ITO region, during spin coating, kapton tape was used, in an initial phase. Figure 3.2 presents the

final outlook of the a) NiO and c) WO_3 films produced with kapton tape. Since kapton tape has hydrophobic properties, the solution presented a natural tendency to move away from the tape during the deposition process, leading to non-uniform films. This effect is more visible in the NiO films, where the region opposite to the ITO contact has a small uniform area. This problem was overcome by making the deposition without protecting the ITO contact with kapton tape and carrying out chemical etching with HCl afterwards. The approximate etching time for both films was around 3 minutes, depending on the age and concentration of the HCl solution. Figure 3.2 shows the optimized b) NiO and d) WO_3 films. Comparing these films with the films produced with kapton tape during spin coating, there is a clear improvement in their uniformity. From figure 3 d) It Is also possible to observe that there was some material accumulation at the borders of WO_3 films due to the spin-coating process.

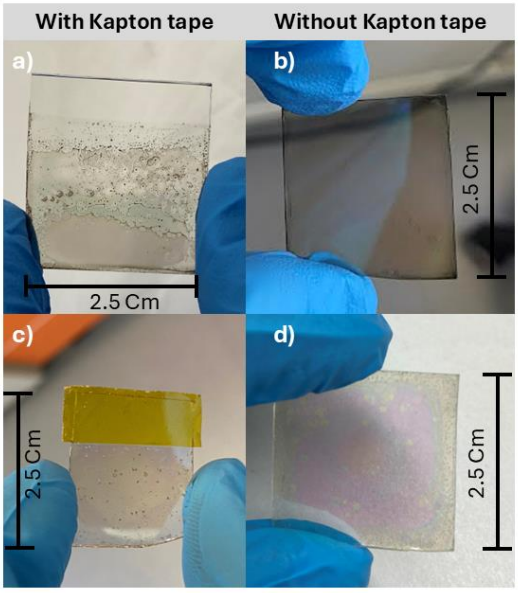

Figure 3.2- Final aspect of NiO and WO3 thin films produced with (a,c) and without (b,d) kapton tape, respectively.

The main concern during chemical etching was to obtain resistance values as close as possible to the ITO resistance, as the contact should be conductive enough to allow insertion/extraction of charges. In order to understand if the obtained values were close to the ITO resistance, it was performed a study of the influence of annealing time in the ITO resistance (Figure 3.3). Has expected, the ITO resistance increased with annealing time, (temperature 300 ºC). Initially the ITO resistance was (25±2) Ω, after 8 stages of 5 minutes of annealing increased to (73±8) Ω

and the sample that remained the same time as the films, 1 hour after the 8 stages of 5 minutes, had an even higher value, (125±28) Ω. For each condition 1 sample was measured.

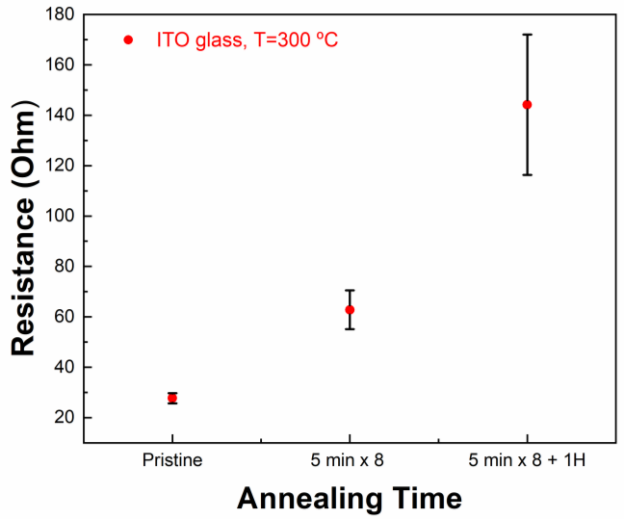

Figure 3.3- Variation of ITO resistance with annealing time

On average the obtained resistance values for the ITO contact after etching, (111±51) Ω for NiO and for WO_3 (116±38) Ω, were slightly lower to the obtained values for the ITO sample that went through the same annealing time, (125±28) Ω, (Figure 3.4). The error bars cover a significant range of values with orders of magnitude that go from the dozens to the hundreds, which might be explained by the quality of the obtained ITO contacts. In most samples there were significant resistance variations trough the contact, the resistance was not the same in different areas possibly due to the presence of some remains of the EC film. Therefore, chemical etching was not uniform trough all ITO contact area. In some samples chemical etching even removed small portions of the ITO, while preserving other regions of the contact. Dry etching is a possible solution to overcome this problem.

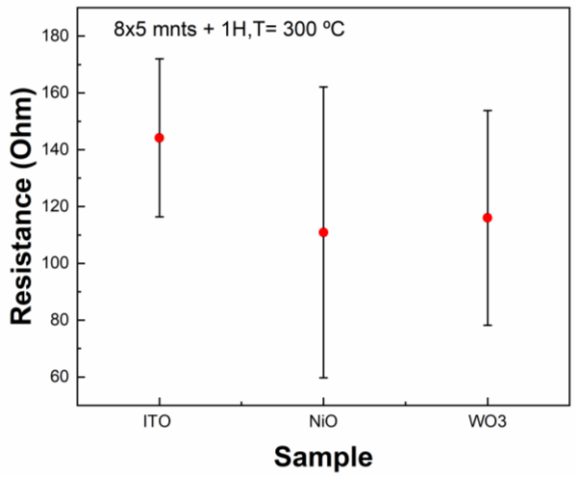

Figure 3.4- Obtained ITO resistance after NiO, WO3 thin films etching and in ITO glass submitted to the same annealing time.

3.2 NiO and WO_3 thin film characterization

The characterization results of the optimized films are presented below as well as a brief discussion. Characterization included profilometry, X-ray diffraction, SEM, FTIR-ATR and UV-Vis-NIR spectroscopy. Lastly, electrochemical characterization included cyclic voltammetry and chronoamperometry measurements, which were made using a potentiostat.

3.2.1 Thickness

The thickness of the EC films was measured with a profilometer and plays an important role on the device's efficiency. The material properties of WO_3 and NiO films vary with film thickness, having impact on their EC performance [21], [26]. NiO thin films presented a thickness of (195±6) nm, much higher than the, (53±3) nm obtained for WO_3, (from an average of 3 samples). Once the spin coater velocity and acceleration were the same for both films, this result can be explained by the different concentration and composition of the precursor solutions.
Profilometer measurements also allowed to understand the profile of the interface between the EC films and the ITO contact. Figure 3.5 presents an example of the profilometer profiles obtained for a) NiO and b) WO_3 films. Both films presented high roughness, which enhances their electrochemical performance but, together with the small thickness of WO_3, made it difficult to measure its value through this technique. AFM measurements should be made to further understand the roughness of the films. Figure 3.5 b) shows a small well at the interface

between the WO_3 film and the ITO contact. In some samples, non-uniform etching led to this situation, preserving the ITO contact while etching the ITO at the interface, damaging the device. These results show a need to further study and improve the NiO and WO3 film's etching to allow for reproducible devices.

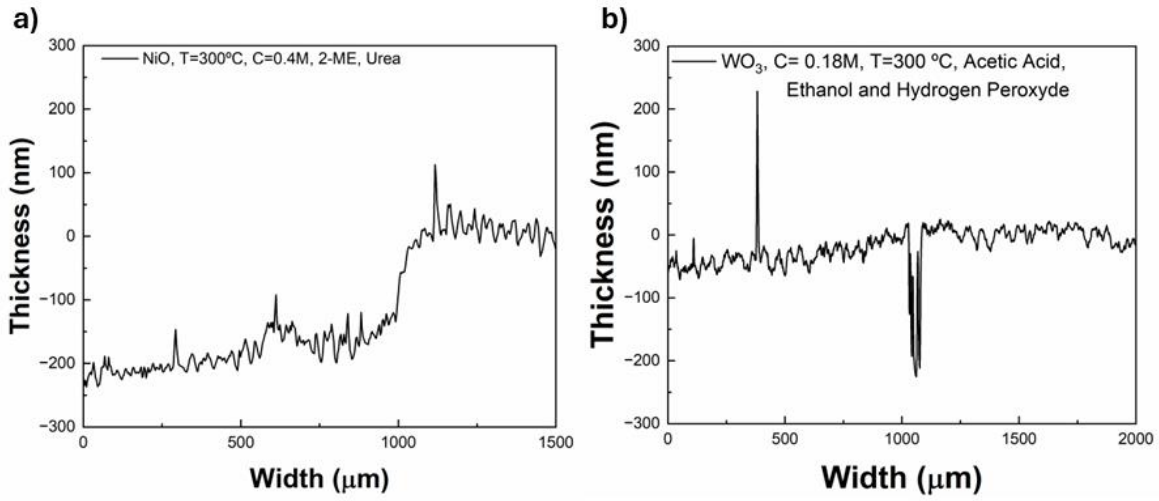

Figure 3.5- Profilometer profiles of a) NiO and b) WO_3 thin films.

3.2.2 X-ray diffraction (XRD)

The crystallographic structure of an EC film has a big influence on its efficiency. Crystalline films have better cyclic stability and better adhesion to the substrate, while amorphous have enhanced switching times and higher coloration efficiencies [2]. The obtained diffractograms are presented in figure 3.6. Both diffractograms revealed the presence of broad bands, rather than the typical sharp peaks of crystalline materials, revealing a short range order for both films. This results are in accordance with a study where WO_3 EC films with different thicknesses were produced by SCS and deposited by spin coating [21]. Samples with less than 150 nm were found to be amorphous, while thicker films presented a polycrystalline structure [21]. The same crystallinity modification with thickness increase has been reported for NiO thin films produced by electron beam evaporation [25]. Therefore, a possible path to increase the crystallinity of the WO_3 films could be by producing samples with thicknesses higher than 150 nm. This could be done by increasing the concentration of the precursor solution or increasing the number of deposited layers. Increasing the concentration of the WO_3 precursor solution trough the same protocol of this work can be challenging, as the reaction is highly exothermic and unstable.

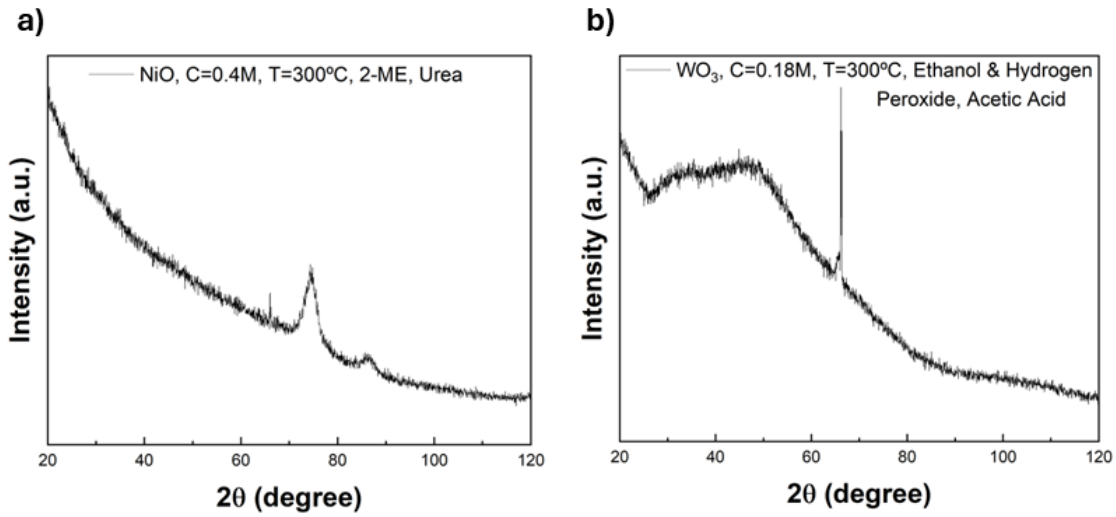

Figure 3.6- X-Ray diffractograms of a) NiO and b) WO_3 films.

3.2.3 Scanning Electron Microscopy (SEM)

As shown in figure 3.7 b), SEM analysis revealed the high porosity of the NiO films. Porous films have an increased contact area between the film and the electrolyte, decreasing the diffusion path of the ions. This will facilitate the charge transfer and, will, therefore, improve the EC properties of the film [2], [8].

SEM images of the NiO films also allowed to verify the absence of cracks on the structure. EDS analysis can be made in the future to understand the composition of the films and verify if NiO is the only element present in the structure.

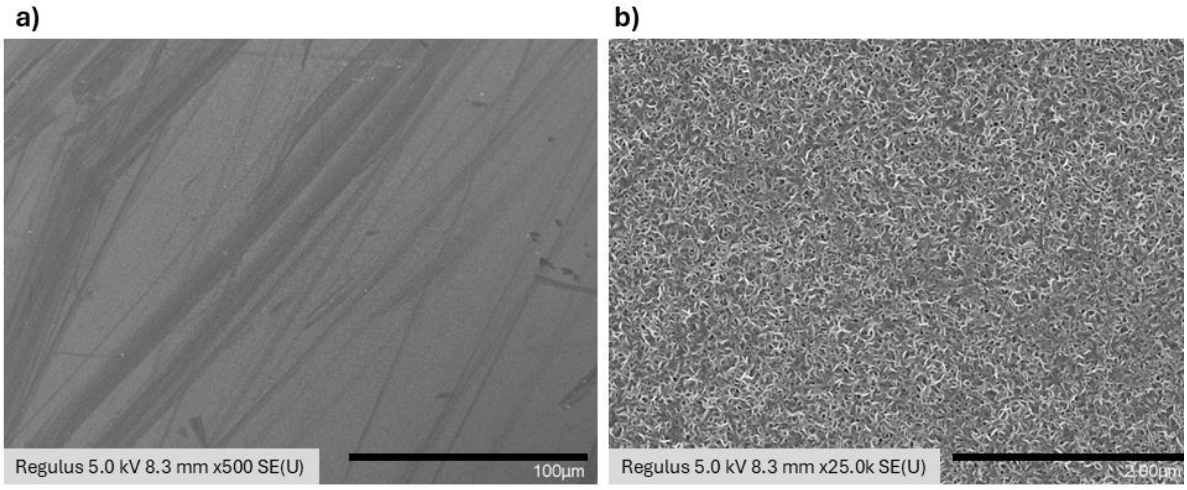

Figure 3.7- SEM Images of NiO films for a magnification of a) x500 and b) x25.0k.

The obtained SEM images of the WO_3 films are presented in figure 3.8 and revealed they did not present any kind of porous structure. The observable white dots can be related to the Au previously deposited to carry the SEM measurements. This result is similar to the previously mentioned report where WO_3 thin films produced by SCS and deposited by spin coating did not present a porous structure [21]. SEM images also show the absence of cracks, which are often reported for WO_3 films that undergo annealing treatments due to the strain imposed by this process [21].

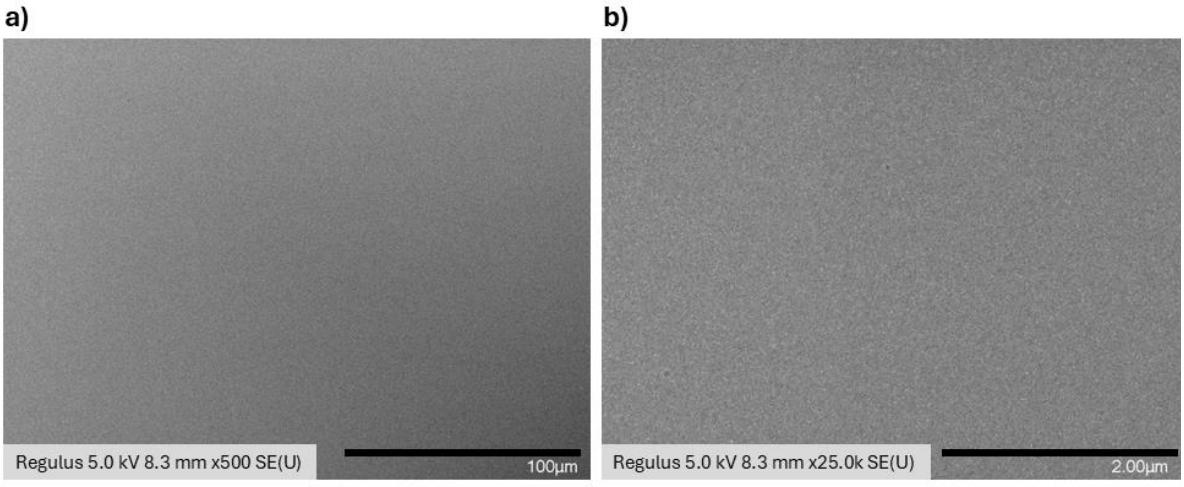

Figure 3.8- SEM Images of WO_3 films for a magnification of a) x500, b)25.0k.

3.2.4 Fourier Transform infrared spectroscopy (FTIR-ATR)

Figure 3.9 shows the obtained FTIR-ATR spectra for both a) NiO and b) WO_3 films deposited in a silicon substrate for samples submitted to the 8 annealing stages of 5 minutes with and without the final 1 hour step. NiO films that were not submitted to the final 1 hour step presented peaks in the hydroxyl region (3432-3672) cm^{-1} (peak 1), and in the nitrate region, (1200-1500) cm^{-1} (peak 2) [26],[27]. The NiO spectra of the films that went through the 1 hour annealing stage did not present this peaks, revealing the importance of this step to convert the metal oxide. The obtained spectra for WO_3 films (figure 3.9 a)) did not present any significant peaks for both conditions, therefore the 8 annealing stages of 5 minutes between layers are enough to convert the metal oxide and the final 1 hour annealing is not relevant to convert to the process.

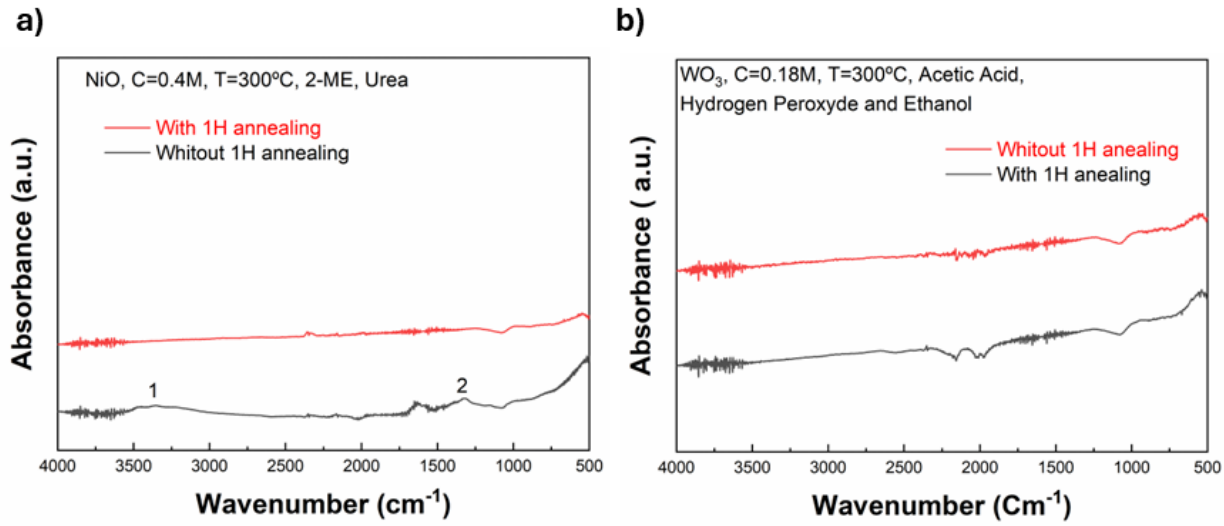

Figure 3.9- FTIR-ATR spectra of a) NiO and b) WO_3 films.

3.2.5 UV-Visible Spectroscopy

Transmittance measurements of the as deposited films on a glass substrate revealed the high transparency of the films, as shown in Figure 3.10. WO_3 films presented a transmittance of 80% (average between 550 nm and 633 nm), while NiO presented a lower value, 65% (average between 550 nm and 633 nm). Most optical modulation values are reported for 550 nm or 633 nm, an average between these values allowed to cover more wavelengths of the visible spectrum.

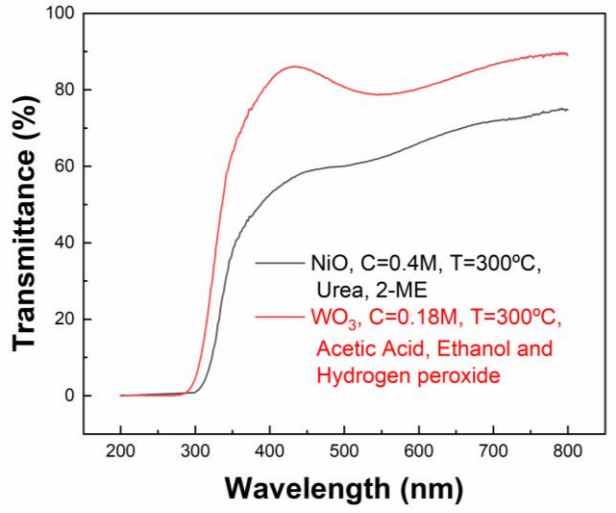

Figure 3.10- Transmittance of NiO and WO_3 thin films on a glass substrate.

To demonstrate the devices performance, voltages of 1 V and -1 V were applied to the ITO contacts of the NiO and WO_3 thin films immersed in the $LiClO_4$ electrolyte. Figure 3.11 presents the obtained spectra from 200 nm to 800 nm for both films in the initial, coloration and bleaching states. From figure 3.11 a) it can be seen that NiO films presented higher transparency after bleaching than at the initial state, and an optical modulation of 20 % ,(average between 550 nm and 633 nm). The reason behind this effect on the NiO films might be related with ion insertion/extraction during the fabrication process that could have led to some intermediate coloration between bleach and coloured states. The optical modulation of NiO films was considerably lower than a recent report of SCS of NiO thin films that used 1 M NaOH as electrolyte, obtaining an optical modulation of 60% (550 nm) [22]. On the other hand, while the annealing stage of this report was made for 3 hours at 450 ºC, in this work annealing was made at a lower temperature, 300 ºC for 8 x 5 minutes between layers and one hour after all.

In figure 3.11 b) it can be seen that, unlike NiO, WO_3 films were more transparent at the initial state than after bleaching and had an optical modulation of 20%, (average between 550 nm and 633 nm). It is interesting to compare the obtained results with a recent study where EC WO_3 spin coated thin films produced by SCS with a thickness of 113 nm and an identical optical modulation of 25% [21]. Once the optical modulation is similar and the thickness is much higher, films produced in this work are more efficient that the reported in the study.

The produced WO_3 films also presented memory effect. After bleaching, it was possible to visually observe the device did not change completely but presented a slightly blue tone (figure 3.13). This effect is common in WO_3 films and can be explain by ion trapping at the films

structure [8]. There are reports of WO_3 films produced at low annealing temperatures leading to the loss of W=O and W-O bonds and creating trapping sites for Li^+ Ions [8]. A stronger discoloration voltage could help overcome this problem, but it could also damage the thin film [8].

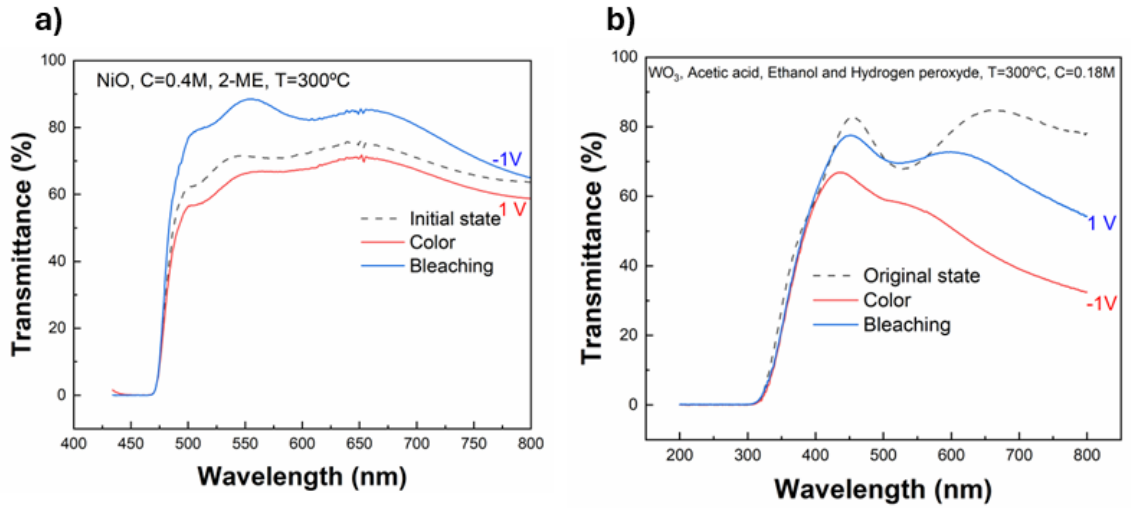

Figure 3.11- Transmittance at initial, coloured and bleached state for a) NiO and b) WO_3 films, for voltages of ±1V. The measurements were performed with a $LiClO_4$ electrolyte (C=0.1M), a platinum counter electrode and a reference electrode.

Figure 3.12 presents the final outlook of the NiO devices produced with kapton tape and through chemical etching. Both coloration and bleaching states were more uniform for the films where the ITO contact was produced through chemical etching, showing a clear improvement in the cells performance.

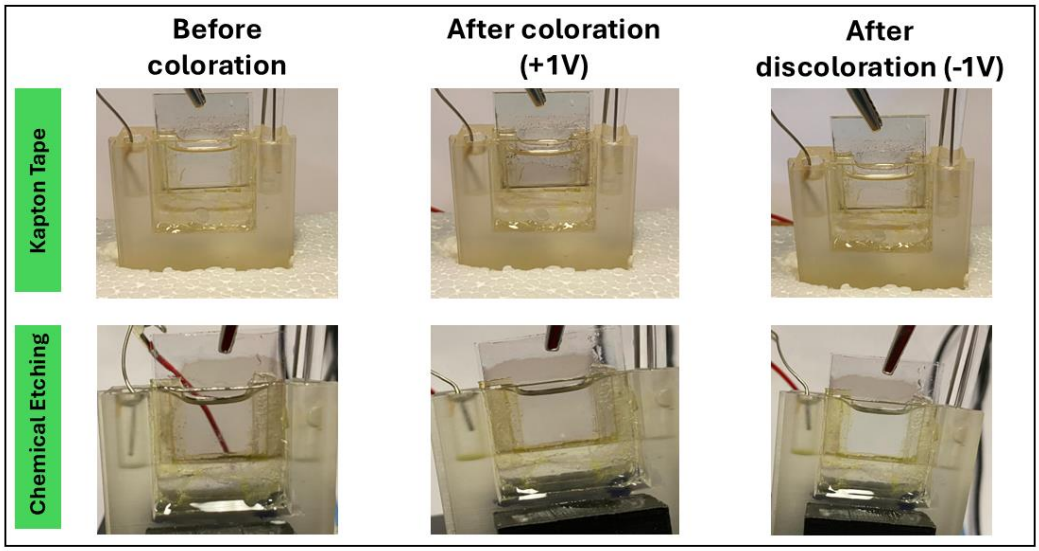

Figure 3.12- Final outlook of NiO films before coloration, after coloration and after discoloration for ±1V.

Figure 3.13 presents the finals aspect of the WO_3 devices produced with kapton tape and trough chemical etching. Both films presented memory effect after discoloration, but films produced through chemical etching presented more uniform coloration and bleaching states. An $LiClO_4$ electrolyte with a concentration of C=0.5M was also tested, but it damaged the film.

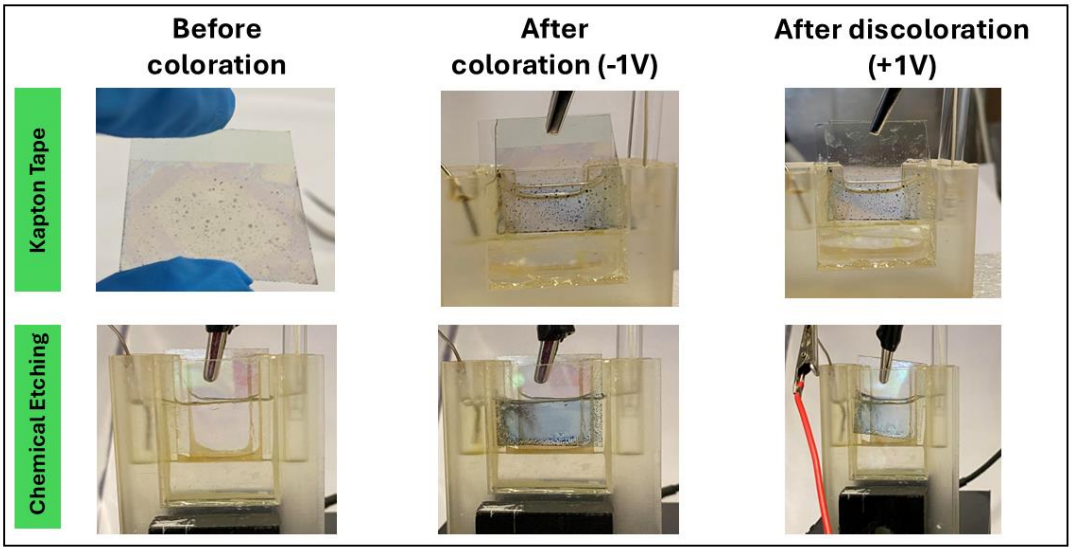

Figure 3.13- Final outlook of WO_3 films before coloration, after coloration and after discoloration for ±1V.

To colour/bleach the devices, as well as to perform the cyclic voltammetry measurements a set up similar to figure 3.14 was used without the portable spectrophotometer, the optical fibers and the light source. The transmittance curves presented in this chapter were measured in a spectrophotometer apart from the set up. The portable spectrophotometer, the optical fibers

and the light source presented in figure 3.14 were used for chronoamperometry measurements.

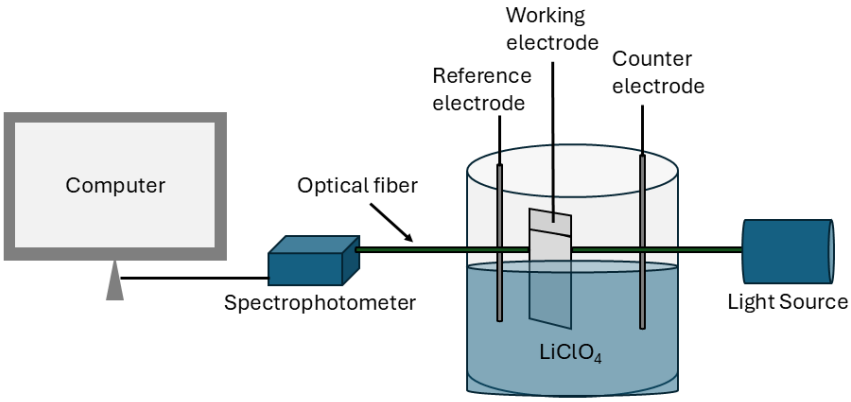

Figure 3.14- Set up used to perform electrochemical measurements. A platinum counter electrode and a LiClO4 electrolyte were used. The electrodes were connected to a potenciostat.

3.2.6 Cyclic Voltammetry

Cyclic Voltammetry is important to understand the cycling stability of the electrochromic films. Figure 3.15 presents the cyclic voltammograms for the first ten cycles for both a) NiO and b) WO_3 films. NiO curves presented two cathodic peaks, 0.4V (I); 0.1mA, 0.9V; 0.16 mA (II) and two anodic peaks, 0.1V;-0.15 mA (I), 0.7V;-0.1 mA (II), therefore having two oxidation states and two reduction states, as depicted in Figure 3.15 a). A recent study has reported similar results for NiO solution based EC films, with two cathodic peaks, 0.3V, 0.9V and two anodic peaks, 0.0V, 0.5V but with double current density [20]. The appearance of two oxidation and two reduction states is typical of NiO films in non aqueous electrolytes like $LiClO_4$, and is explained by the double injection and extraction of charges [2].

As the cycles draw near the 10^{th}, the current increases and tends to stabilize. Therefore, since the area under the CV curves represents the charge storage capacity of the films, the EC behaviour increase as the cycle draw near the 10^{th} due to an increased capacity to store charges. This phenomenon could be explained as an activation step, being a typical behaviour of NiO devices with aqueous electrolytes [2]. There are reports of a significant increase of charge capacity that can last the first hundred cycles [2]. This behaviour did not occur with WO_3 thin films as their peak current density remained stable trough the cycles.

WO_3 curves only presented one cathodic peak at 0.1V, 0.6mA (I) as shown in Figure 3.15 b). Once the coloration/bleaching mechanism is based on a redox process, a cathodic peak was expected to appear, completing the redox cycle. If the cycles covered more negative values, surpassing -1.5 V, the cathodic peak would appear, but once the device could get damaged,

higher voltages where not explored. During the bleaching process, WO_3 films presented a current of 0.49 mA, more than the double of NiO 0.15 mA, meaning more charges were injected into the WO_3 when compared with NiO thin films.

The obtained WO_3 cycles match the results of an already mentioned study where WO_3 films with thicknesses from 41 nm to 750 nm were produced trough SCS [21]. For 41 nm films, the study reported an anodic peak current of 0.20 mA, against 0.26 mA of this work, where the films had 53 nm [21]. Therefore, this work was able to obtain a similar current with a slightly higher thickness.

The area under the curves of NiO is bigger than under the WO_3, consequently NiO films have more capacity to store charges than WO_3, leading to a higher efficiency, this can be explained by the higher porosity of the NiO devices.

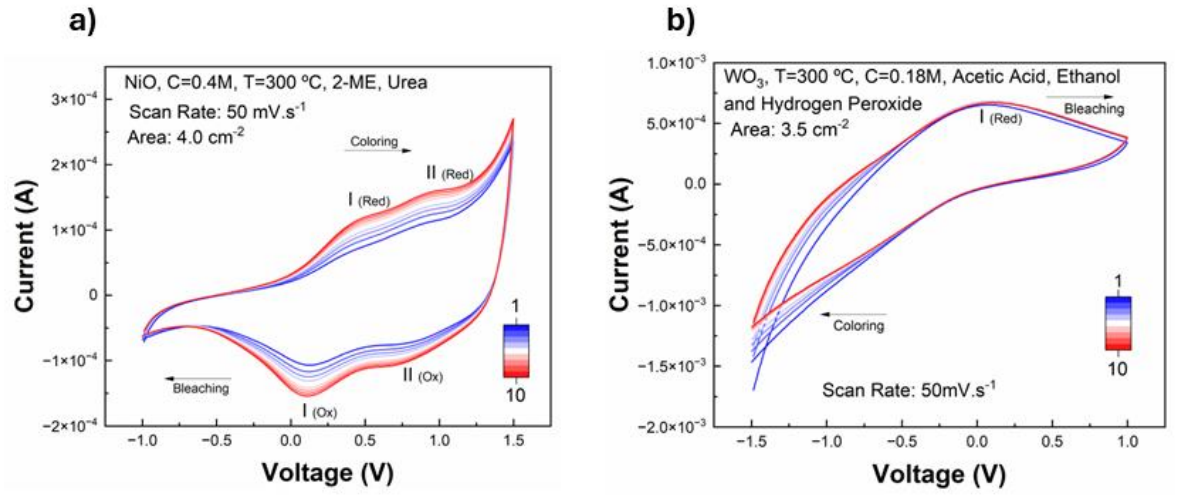

Figure 3.15- First 10 cyclic voltammetry cycles for a) NiO and b) WO_3 cells. The measurements were made with a $LiClO_4$ electrolyte and a platine counter electrode.

3.2.7 Chronoamperometry

Chronoamperometry curves allowed to calculate the coloration/bleaching times of the films as well as to understand the optical modulation variation trough the coloration/bleaching cycles. Figure 3.16 a) presents the obtained results for NiO films during 15 cycles. The applied coloration/bleaching voltages were 1V/-0.5V respectively. As shown in figure 3.16 b), transmittance in both coloured and bleached states increased until the 5^{th} cycle, when it stabilizes. Through this process the optical modulation remains practically the same. This might be explained by the same activation step that led to an increase of current and prior stabilization during cyclic voltammetry. Coloration/Bleaching times are defined as the necessary time for a 90%

coloration/bleaching variation to occur [6]. These times were extracted from the final 5 cycles, (figure 3.16 b)) since the curves were more stable. NiO films presented a coloration time ($t_{C,90\%}$) of (21±1) s and a bleaching time of ($t_{B,\ 90\%}$) (8±1) s. A recent study reported coloration/bleaching times of 17/2s, although the obtained results did not surpass these times, they are still acceptable for EC windows [20]. The protocol followed by the study evolved a 24 hours drying stage followed by annealing at 230 ºC for 90 minutes while this work only had 8 stages of 5 minutes between layers and one hour after hall [20].

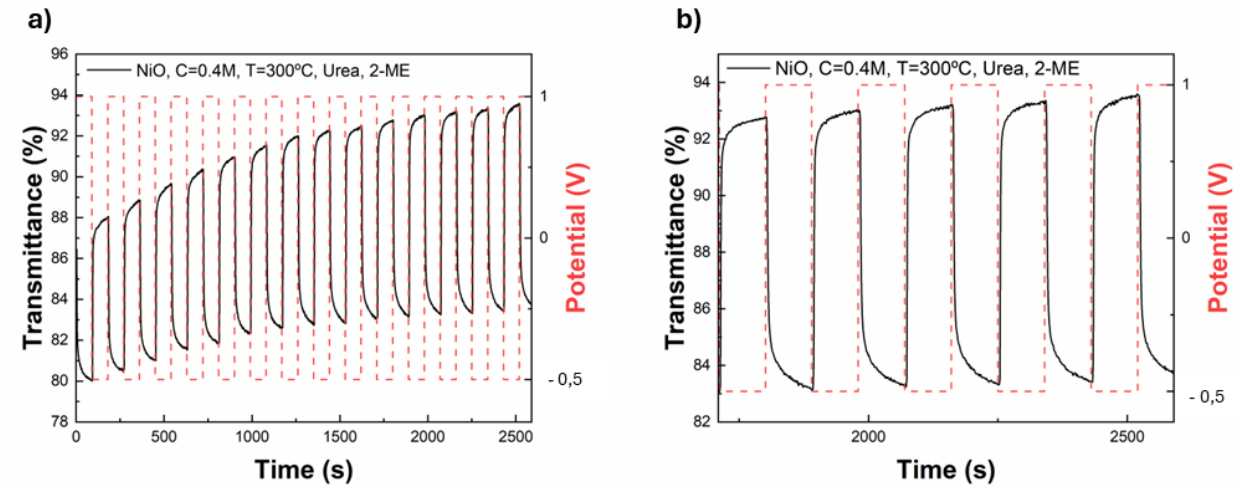

Figure 3.16- Chronoamperometry measurements of anodic NiO cells for a) the first 15 cycles, b) the final 5 cycles.

Figure 3.17 a) presents the chronoamperometry results for WO_3 films for the first 15 cycles, where voltages of -1.5 V and -0.25 V were applied for coloration/bleaching. While optical modulation remains constant, the transmittance in both colour and bleach state decreased continuously until the 10^{th} cycle, where it stabilized. A possible cause can be the previously mentioned capture of electrolyte Li^+ ions by the film structure that leads to an Irreversible colour change [8]. This phenomenon has been appointed as the main degradation reason of the EC performance for WO_3 devices[8]. Potentiostatic conditioning of the films has been indentified has a possible technique to improve the reversibility of the coloration/bleaching process, improving the performance of the films affected by this problem [8]. Similarly to NiO, coloration/bleaching times for WO_3 films were calculated for the final 5 cycles (figure 3.17 b)), where the curves were more stable. WO_3 films presented a coloration time ($t_{c,90\%}$) of (45±7) s and a bleaching time ($t_{b,90\%}$) of (46±4) s. Recent studies of WO_3 solution based spin coated EC films reported lower

coloration/bleaching times of 20s/5s for films with 113nm thickness or even 36s/13s for films with 456 nm of thickness [21]. Another study reported the production of WO_3 films by self-assembly with coloration/bleaching times of 86 s/78 s, which are much higher than the (45±7) s/(46±4) s obtained in this work [16]. Comparing WO_3 and NiO switching times, even with a higher thickness, NiO films ((195±6) nm) take less time to colour/bleach (21±1) s/(8±1) s than WO_3 ((53±3) nm), (45±7) s/(46±4) s.

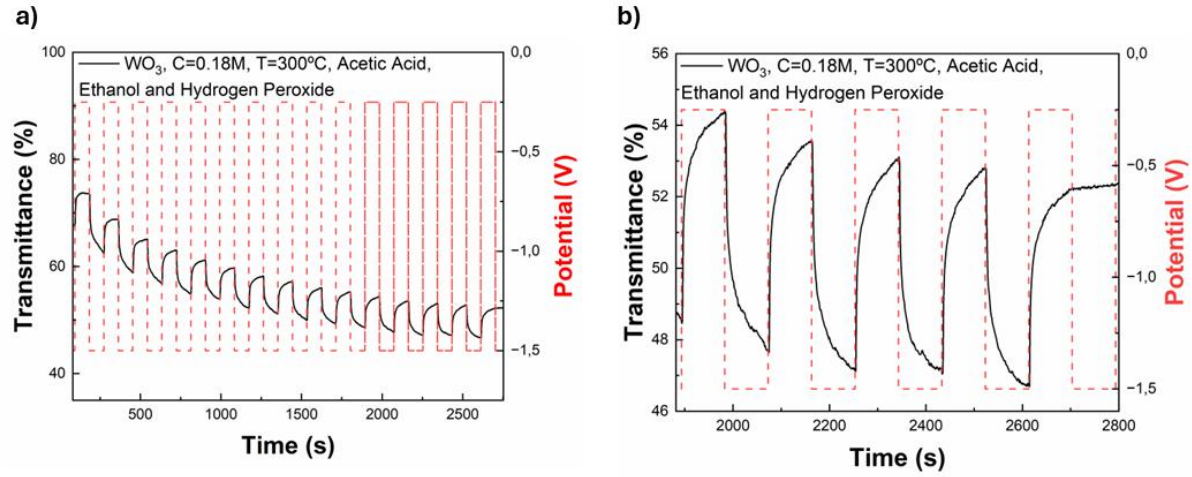

Figure 3.17- Chronoamperometry measurements of cathodic WO_3 cells for a) the first 15 cycles b) the final 5 cycles.

The optical modulation values obtained with chronoamperometry measurements did not match the ones obtained when testing the device's performance, (where the transmittance was measured in a separate spectrophotometer). This effect might be explained by the setup of the chronoamperometry measurements, therefore the values presented in figure 3.11 are more reliable and were used to compare with the reported literature. Nevertheless, these results allowed to verify that there were reversible coloration/bleaching cycles as well as to calculate the coloration/bleaching times.

Table 3.1 presents the state of the art for NiO and WO_3 solution based EC devices, as well as the results obtained in this work.

Although the EC properties of the produced NiO and WO_3 films were lower than most results reported in literature, this work reached acceptable properties for application in EC devices through a simpler and low-cost method.

Table 3.1- Comparison between state of the art of solution-based NiO and WO3 EC devices and the results obtained in this work

	Method/ Structure	Electrolyte	CE ($Cm^2.C^{-1}$)	ΔT (%)	Coloration/ Bleaching Times (s)	Ref
WO_3	Combustion	1M LiClO4-PC	56	556 (633 nm)	6/3	[24]
		1 M LiI-PEG	35	40 (633 nm)	32/10	[25]
	Spray Coating	0.2 MLiClO4-PC	77	98 (633 nm)	5/4	[18]
	Inkjet Printing	61:17:7:15 ACN:PC:LiClO4:PMMA	132	75 (633 nm)	10/13	[17]
	Self assembly	0.1M LiClO4-PC	121	61.4 (1060 nm)	86/78	[16]
	This Work	0.1 M LiClO4	-	20 (550-633) nm	45/46	-
NiO	Sol Gel	1 M KOH	71	51 (550 nm)	-	[12]
	Spray Pyrolysis	0.5 M PC-LiClO4	31	39 (550 nm)	8/2	[11]
	Combustion	1 M NaOH	26	60 (550 nm)	11.8/4	[22]
		1 M $LiClO_4$	92	55 (550 nm)	17/2	[20]
	This Work	0.1 M LiClO4	-	20 (550-633) nm	21/8	-

Once both films presented a reversible electrochromic behaviour, it would be interesting to combine them in a complementary effect electrochromic window. Voltages between -1V and 1V could be tested, once they did not damaged the devices produced in this work.

4

CONCLUSION AND FUTURE PERSPECTIVES

The objective of this work was to produce and characterize solution combustion synthesis based NiO and WO_3 EC films deposited by spin coating. The first spin coating depositions were made with a small region of the ITO glass covered with kapton tape to preserve a contact conductive enough to allow charge insertion/extraction. The metal oxide thin films produced through this method were not uniform and a second production method was explored by making the deposition without the tape and proceeding with HCl chemical etching afterwards. To assist the chemical etching, a study of the influence of annealing time in the ITO resistance was performed. It was observed a resistance increase with the annealing time, from (25±2) Ω, prior to the process, to (125±28) Ω, after 8 stages of 5 minutes plus 1 hour.

Optimized NiO and WO_3 thin films were structurally, optically and electrochemically characterized. X-ray diffraction analysis revealed the lack of long-range order in both films, while SEM analysis disclosed NiO films were porous and WO_3 films were not. NiO films presented higher thickness, (195±6) nm, than WO_3, (53±3) nm, and an identical optical modulation of 20% . However, these values are lower than most results reported in the literature. For NiO films, Cyclic voltammetry showed that as the cycles draw near the 10^{th}, the injected current increased and tended to stabilize. NiO films presented two cathodic peaks at 0.4V (I); 0.1mA, 0.9V; 0.16 mA (II) and two anodic peaks at 0.1V;-0.15 mA (I), 0.7V;0.1 mA (II). While WO_3 films only presented one cathodic peak at 0.1V, 0.6mA (I). Although the obtained peak currents were lower than most results reported in the literature, it was achieved a reversible EC behaviour, for both films. Chronoamperometry measurements allowed to calculate the coloration/bleaching times. NiO films presented coloration/bleaching times of (21±1) s/(8±1) s and WO_3 of (45±7) s/(46±4). These times are higher than most literature reports, but are acceptable for application in EC windows.

Although the electrochromic performance of the produced films was lower than most solution-based NiO and WO_3 EC devices reported in literature, this work was able to produce NiO and WO_3 films with reversible EC performance through a number of cycles, by a simple protocol.

To continue this work, chronoamperometry measurements could be made until the 1000^{th} cycle to further understand the lifecycle of both films. A possible path to enhance the performance of the WO_3 EC films presented in this work could be to increase their thickness. Another relevant path to follow could also be to reproduce the obtained results with a solid electrolyte, once it would overcome the leakage problem of liquid electrolytes. Finally, since both films presented the ability to colour/bleach at similar voltages, both films could be combined in a complementary effect electrochromic window.

To conclude, SCS proved to be a simple method capable of producing reversible EC films, therefore it is important to continue this work once it can help lowering the production costs of NiO and WO_3 EC devices.

BIBLIOGRAPHY

[1] K. Calvin *et al.*, "IPCC, 2023: Climate Change 2023: Synthesis Report. Contribution of Working Groups I, II and III to the Sixth Assessment Report of the Intergovernmental Panel on Climate Change [Core Writing Team, H. Lee and J. Romero (eds.)]. IPCC, Geneva, Switzerland.," Jul. 2023. doi: 10.59327/IPCC/AR6-9789291691647.

[2] F. Zhao *et al.*, "Nickel oxide electrochromic films: mechanisms, preparation methods, and modification strategies-a review," Apr. 03, 2024, *Royal Society of Chemistry*. doi: 10.1039/d4tc00114a.

[3] C. Göran Granqvist, "Electrochromic Metal Oxides: An Introduction to Materials and Devices" in Electrochromic Materials and Devices, Roger J. Mortimer, David R. Rosseinsky and Paul M. S. Monk, first edition, 2015

[4] D. Zhou, D. Xie, X. Xia, X. Wang, C. Gu, and J. Tu, "All-solid-state electrochromic devices based on WO3||NiO films: material developments and future applications," Jan. 01, 2017, *Science in China Press*. doi: 10.1007/s11426-016-0279-3.

[5] Chua. M, Tang. T, Ong. K, Neo. W, Xu. J "Introduction to Electrochromism." in Electrochromic Smart Materials: Fabrication and Applications, Xu. J, Chua. M, Shah. K, 2019

[6] C. Gu, A. B. Jia, Y. M. Zhang, and S. X. A. Zhang, "Emerging Electrochromic Materials and Devices for Future Displays," Sep. 28, 2022, *American Chemical Society*. doi: 10.1021/acs.chemrev.1c01055.

[7] Y. Ding, M. Wang, Z. Mei, and X. Diao, "Different ion-based electrolytes for electrochromic devices: A review," Dec. 01, 2022, *Elsevier B.V.* doi: 10.1016/j.solmat.2022.112037.

[8] J. Y. Zheng *et al.*, "Review on recent progress in WO3-based electrochromic films: preparation methods and performance enhancement strategies," Nov. 09, 2022, *Royal Society of Chemistry*. doi: 10.1039/d2nr04761f.

[9] G. Cai, P. Darmawan, M. Cui, J. Chen, X. Wang, A. L. S. Eh, S. Magdassi and P. S. Lee, Nanoscale, " Inkjet-printed all solid-state electrochromic devices based on NiO/WO3 nanoparticle complementary electrodes", 2016, 8, 348–357, doi: 10.1039/c5nr06995e.

[10] K. Xu, L. Wang, S. Xiong, C. Ge, L. Wang, B. Wang, W. Wang, M. Chen and G. Liu, Electro chim. Acta, "A high-performance electrochromic device assembled with WO3/Ag and TiO2/NiO composite electrodes towards smart window", 2023, 441, 141812, doi: 10.1016/j.electacta.2023.141812 .

[11] J. Denayer, G. Bister, P. Simonis, P. Colson, A. Maho, P. Aubry, B. Vertruyen, C. Henrist, V. Lardot, F. Cambier and R. Cloots, Appl. Surf. Sci., "Surfactant-assisted ultrasonic spray pyrolysis of nickel oxide and lithium-doped nickel oxide thin films, towards electro chromic applications", 2014, 321, 61.7, doi: 10.1016/j.apsusc.2014.09.128.

[12] K. Zhou, Z. Qi, B. Zhao, S. Lu, H. Wang, J. Liu and H. Yan, Surf. Interfaces, "High-Performance Electrochromic NiO Films by Sol-Gel Process", 2017, 6, 91, doi: 10.1016/j.surfin.2017.06.004.

[13] J. R. A. Acunã, I. Perez, V. Sosa, F. Gamboa, J. T. Elizalde, R. Farı´as, D. Carrillo, J. L. Enrı´quez, A. Burrola and P. Mani, Optik, " Sputtering power effects on the electro chromic properties of NiO films", 2021, 231, 166509, doi: 10.1016/j.ijleo.2021.166509.

[14] Y. Li, W. A. McMaster, H. Wei, D. Chen and R. A. Caruso, ACS Appl. Nano Mater., "Enhanced Electrochromic Properties of WO_3 Nanotree-Like Structures Synthesized via a Two-Step Solvothermal Process Showing Promise for Electrochromic Window Applications", 2018, 1, 2552–2558, doi: 10.1021/acsanm.8b00190.

[15] J. Pan, Y. Wang, R. Zheng, M. Wang, Z. Wan, C. Jia, X. Weng, J. Xie and L. Deng, J. Mater. Chem. A, 2019, 7, 13956–13967, "Directly grown high-performance WO_3 films by a novel one-step hydrothermal method with significantly improved stability for electrochromic applications", doi: 10.1039/C9TA01681E.

[16] H. Gu, C. Guo, S. Zhang, L. Bi, T. Li, T. Sun and S. Liu, ACS Nano, 2018, 12, 559–567, doi: 10.1039/d2nr04761f.

[17] G. Cai, P. Darmawan, M. Cui, J. Chen, X. Wang, A. L. S. Eh, S. Magdassi and P. S. Lee, Nanoscale, " Inkjet-printed all solid-state electrochromic devices based on NiO/WO3 nanoparticle complementary electrodes", 2016, 8, 348–357, doi: 10.1039/c5nr06995e.

[18] Y. Yao, Q. Zhao, W. Wei, Z. Chen, Y. Zhu, P. Zhang, Z. Zhang and Y. Gao, Nano Energy, " WO3 quantum-dots electrochromism", doi: 10.1016/j.nanoen.2019.104350.

[19] Y. Zhao, X. Zhang, X. Chen, W. Li, L. Wang, F. Ren, J. Zhao, F. Endres and Y. Li, ACS Sustainable Chem. Eng., 2020, 8, 11658–11666, doi: 10.1039/d2nr04761f.

[20] C. Lupo, F. Eberheim, and D. Schlettwein, "Facile low-temperature synthesis of nickel oxide by an internal combustion reaction for applications in electrochromic devices," *J Mater Sci*, vol. 55, no. 29, pp. 14401–14414, Oct. 2020, doi: 10.1007/s10853-020-04995-8.

[21] B. Wen-Cheun Au, K. Y. Chan, and D. Knipp, "Effect of film thickness on electrochromic performance of sol-gel deposited tungsten oxide (WO3)," *Opt Mater (Amst)*, vol. 94, pp. 387–392, Aug. 2019, doi: 10.1016/j.optmat.2019.05.051.

[22] K. K. Chiang and J. J. Wu, "Fuel-assisted solution route to nanostructured nickel oxide films for electrochromic device application," *ACS Appl Mater Interfaces*, vol. 5, no. 14, pp. 6502–6507, Jul. 2013, doi: 10.1021/am400192s.

[23] E. Carlos, R. Martins, E. Fortunato, and R. Branquinho, "Solution Combustion Synthesis: Towards a Sustainable Approach for Metal Oxides," Jul. 27, 2020, *Wiley-VCH Verlag*. doi: 10.1002/chem.202000678.

[24] X. Huo, H. Zhang, W. Shen, X. Miao, M. Zhang and M. Guo, J. Mater. Chem., " Bifunctional aligned hexagonal/amorphous tungsten oxide core/shell nanorod arrays with enhanced electrochromic and pseudocapacitive performance", A, 2019, 7, 16867–16875, doi: 10.1039/C9TA03725J.

[25] D. R. Sahu, T. J. Wu, S. C. Wang, and J. L. Huang, "Electrochromic behavior of NiO film prepared by e-beam evaporation," *Journal of Science: Advanced Materials and Devices*, vol. 2, no. 2, pp. 225–232, Jun. 2017, doi: 10.1016/j.jsamd.2017.05.001.

[26] A. Adamczyk and E. Długoń, "The FTIR studies of gels and thin films of Al 2O 3-TiO 2 and Al 2O 3-TiO 2-SiO 2 systems," *Spectrochim Acta A Mol Biomol Spectrosc*, vol. 89, pp. 11–17, Apr. 2012, doi: 10.1016/j.saa.2011.12.018.

[27] F. Gan, K. Wu, F. Ma, and C. Du, "In Situ Determination of Nitrate in Water Using Fourier Transform Mid-Infrared Attenuated Total Reflectance Spectroscopy Coupled with De-convolution Algorithm," *Molecules*, vol. 25, no. 24, Dec. 2020, doi: 10.3390/MOLECULES25245838.

[28] S. L. González-Cortés and F. E. Imbert, "Fundamentals, properties and applications of solid catalysts prepared by solution combustion synthesis (SCS)," Feb. 15, 2013. doi: 10.1016/j.apcata.2012.11.024.

A

ANNEXES

A.1 Stoichiometric calculations

The stoichiometric calculations made to find the stoichiometry of the two redox reactions that led to the formation of NiO and WO_3 are presented below. Table A1 presents the valence calculations for each reagent. Propellant chemistry determines a valence of +4 for carbon, +1 for hydrogen, 0 for nitrogen, -2 for oxygen [28].

Table A1- Calculation of the valence of the reagents according to propellant chemistry.

Reagent	Chemical Formula	Calculation	Total
OV	$Ni(NO_3)_2.6H_2O$	$2+2\times(0+3\times(-2))$	-10
	H_2O_2	2 +2x (-2)	-2
RV	$CO(NH_2)_2$	$4+(-2)+2\times(0+2\times1)$	6
	CH_3COOH	$4+3\times1+4+2\times(-2)+1$	8

The molar stoichiometry required to achieve a stoichiometric redox reaction (Φ=1) is obtained by dividing the oxidising and the reducing valences, as shown in table A2.

Table A2-Molar stoichiometry of reagents for Φ=1

Metal Source	Fuel	Φ	n
Nickel Nitrate	Urea	1	$\frac{5}{3}$
Hydrogen peroxide	Acetic Acid	1	$\frac{1}{4}$

Table A3 presents the chemical equations with the calculated stoichiometry.

Table A3- Redox reactions with the stoichoimetry.

Metal Source	Fuel	Solvent	Reaction
Nickel Nitrate	Urea	2-ME	$3Ni(NO_3)_2.6H_2O + 5CO(NH_2)_2 \overset{\Delta T}{\rightarrow} 3NiO + 8N_2 + 28H_2O + 5CO_2$
Tungsten Hexachloride	Acetic Acid	Ethanol and Hydrogen Peroxide	$WCl_6 + CH_3COOH + 4H_2O_2 \overset{\Delta T}{\rightarrow} WO_3 + 6HCl + 4H_2O + 2CO_2$